Supplement of Atmos. Chem. Phys., 26, 5617–5634, 2026
https://doi.org/10.5194/acp-26-5617-2026-supplement

Atmospheric Chemistry and Physics
Open Access
EGU

Supplement of

Seasonal variability and cloud-type effects on secondary organic aerosol formation during cloud events at a mountainous site in southeastern China

Yi Zhang et al.

Correspondence to: Weiqi Xu (xuweiqi@mail.iap.ac.cn) and Yele Sun (sunyele@mail.iap.ac.cn)

S1. Backward trajectory model

In order to examine the origins and transport routes of air masses reaching the SH site during cloud events, backward trajectory modelling was conducted using the Hybrid Single Particle Lagrangian Integrated Trajectory (HYSPLIT) model (Stein et al., 2015). The HYSPLIT model calculated 36-hour backward trajectories of air masses at every hour for each cloud events, using an endpoint height of 1100 m above sea level. The backward trajectories analysis was performed using MeteoInfo, a software developed by Wang (2014). This software facilitated the efficient calculation and visualization of the backward trajectory results.

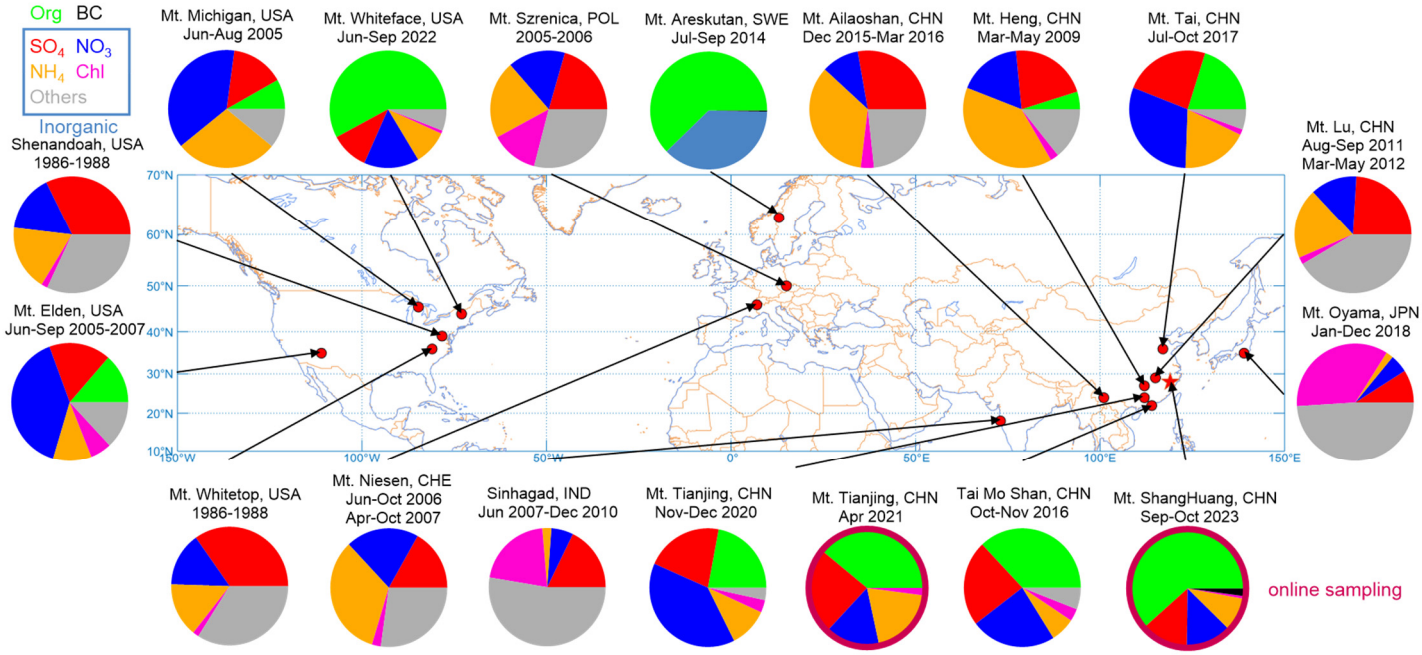

Figure S1: Chemical composition of cloud water and cloud residuals (red circle) sampled at the high-altitude stations all over the world. This measurement is marked as a pentagram on the map.

Figure S2: Photographic documentation of meteorological conditions during the 2023 field campaign.

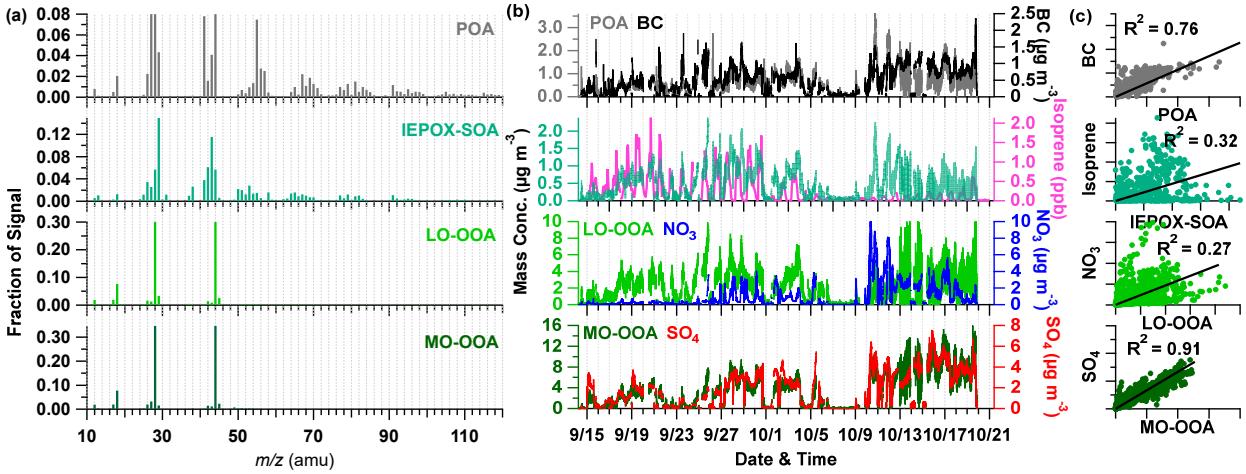

Figure S3: (a) Time series and (b) mass spectral profiles of four OA factors (POA, IEPOX-SOA, LO-OOA and MO-OOA) of the measurement in the autumn of 2023 determined by PMF analysis. The time series of external tracers (BC, isoprene, NO_3 and SO_4) and (c) correlations are also shown for comparison.

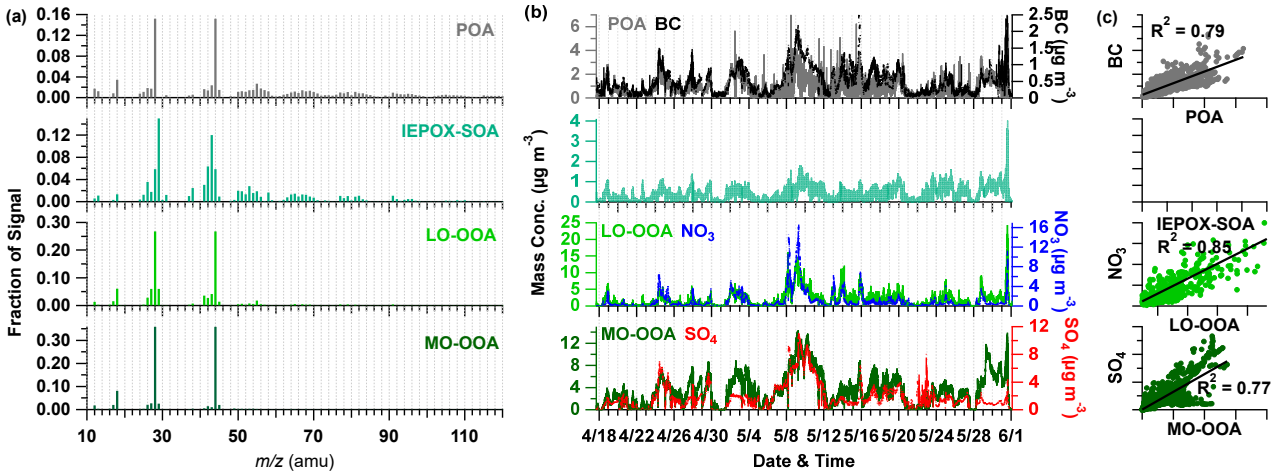

Figure S4: (a) Time series and (b) mass spectral profiles of four OA factors (POA, IEPOX-SOA, LO-OOA and MO-OOA) of the measurement in the spring of 2024 determined by PMF analysis. The time series of external tracers (BC, isoprene, NO_3 and SO_4) and (c) correlations are also shown for comparison.

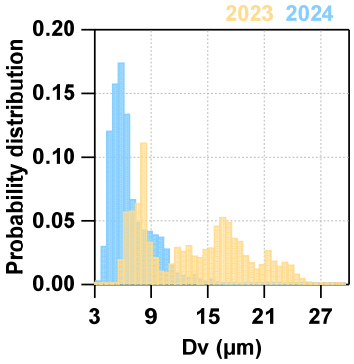

Figure S5: Average probability distribution of D_v during the cloud periods in 2023 and 2024.

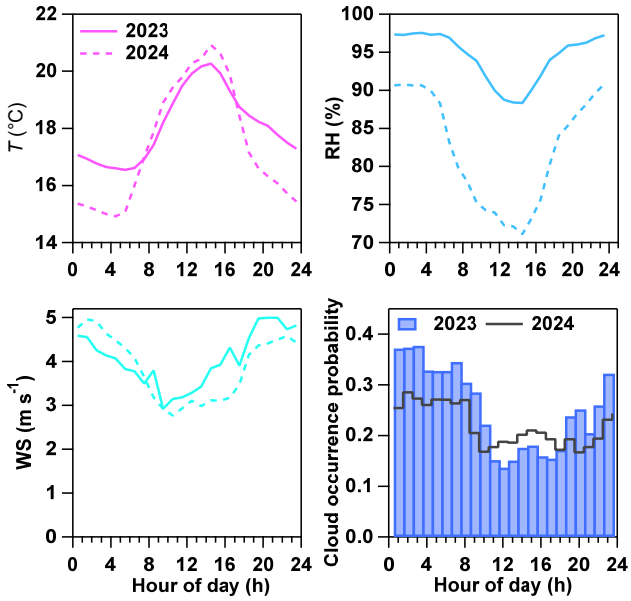

Figure S6: Diurnal pattern of meteorological parameters during the SH field campaign in both 2023 and 2024.

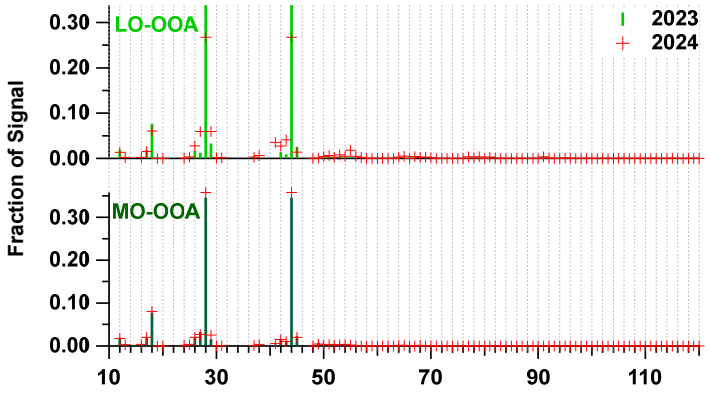

Figure S7: Comparison of OA factor spectra (LO-OOA and MO-OOA) resolved in 2023 and 2024.

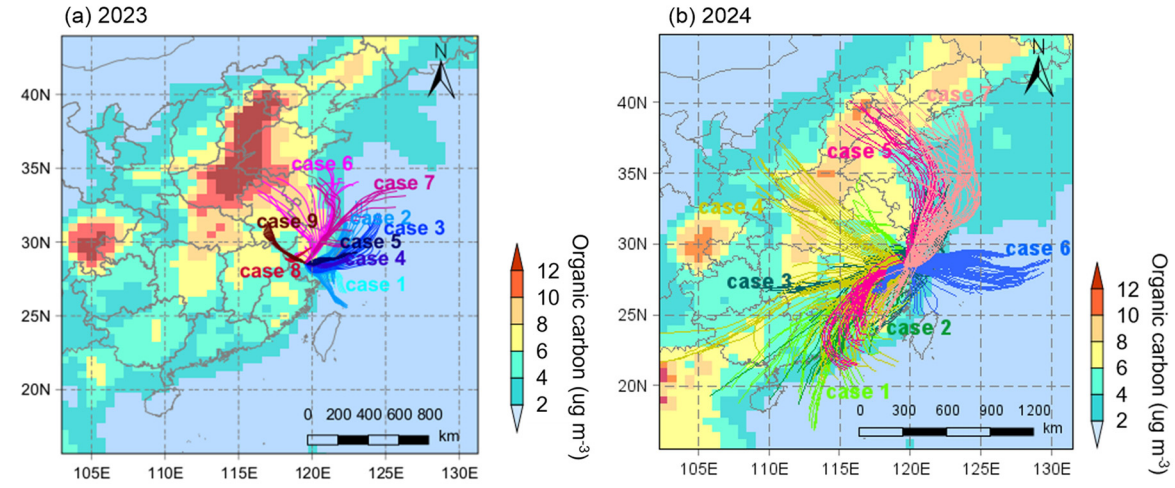

Figure S8: Back trajectories calculated at 1-hour intervals during cloud events at the SH site in (a) 2023 and (b) 2024.

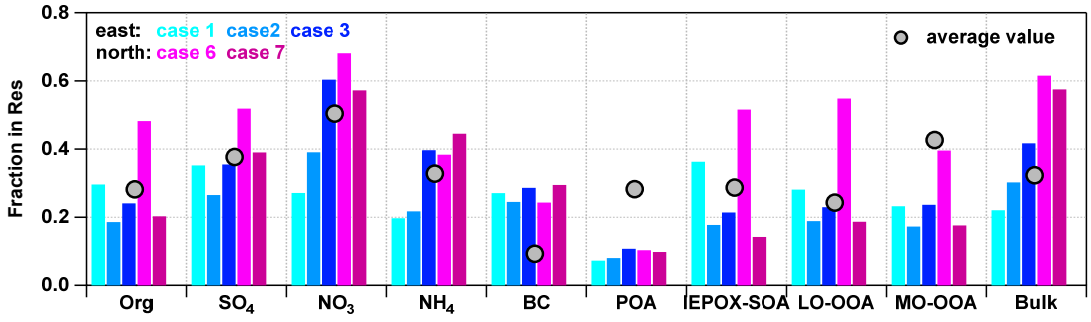

Figure S9: Average fraction of chemical components in Res particles during every cloud event in 2023. All cloud events are grouped in colour based on their air masses sources.

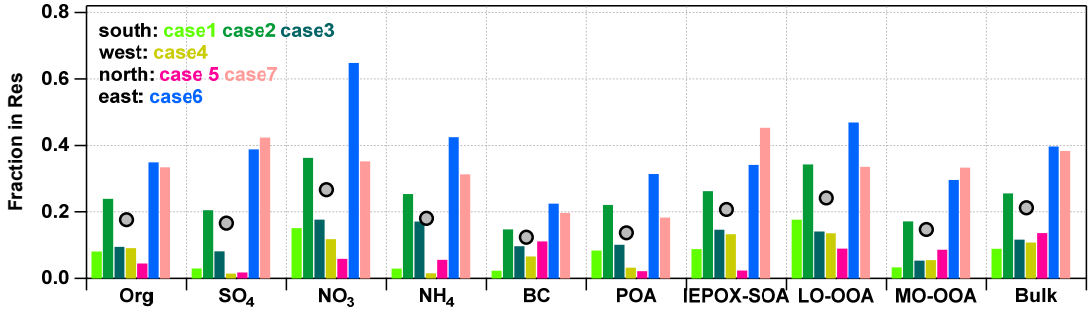

Figure S10: Average fraction of chemical components in Res particles during every cloud event in 2024. All cloud events are grouped in colour based on their air masses sources.

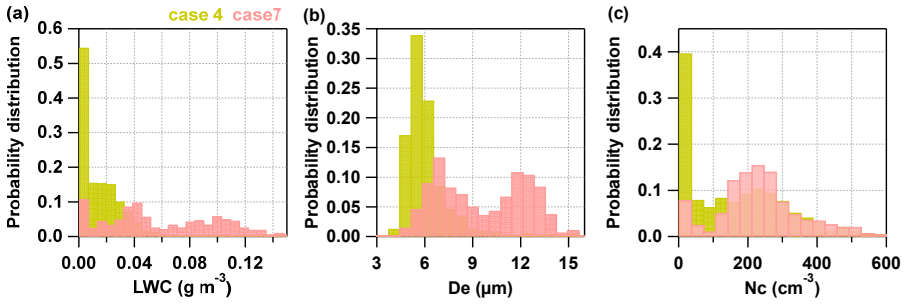

Figure S11: Comparison of cloud microphysical parameters between case 4 and case 7 in 2024.

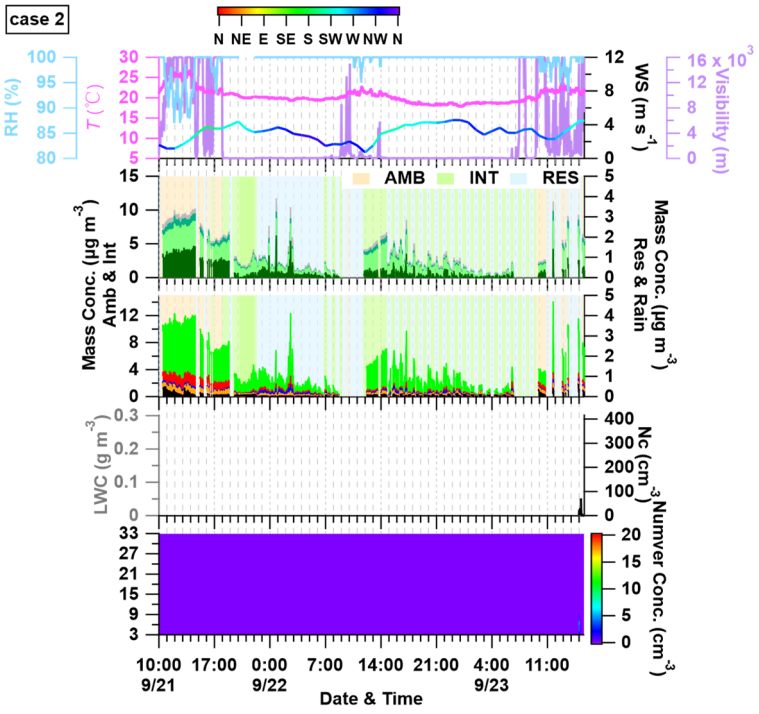

Figure S12: The evolution of meteorological variables (*T*, RH, wind, and visibility), OA factors (POA, IEPOX-SOA, LO-OOA, and MO-OOA), chemical composition (Org, SO4, NO3, NH4, Chl, BC) and cloud microphysical parameters (LWC and Nc) during cloud case 2 in 2023.

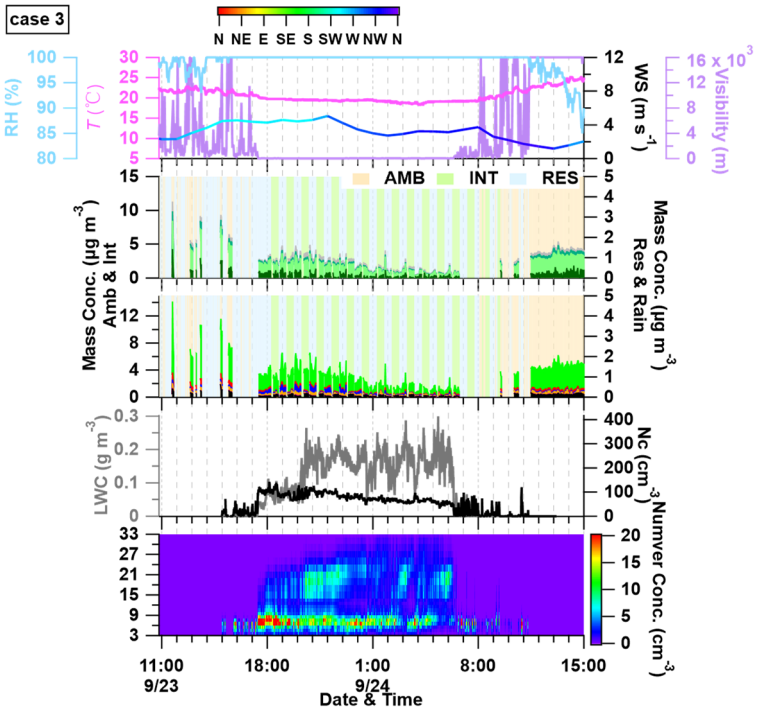

Figure S13: Same as Fig. S12, but for cloud case 3 in 2023.

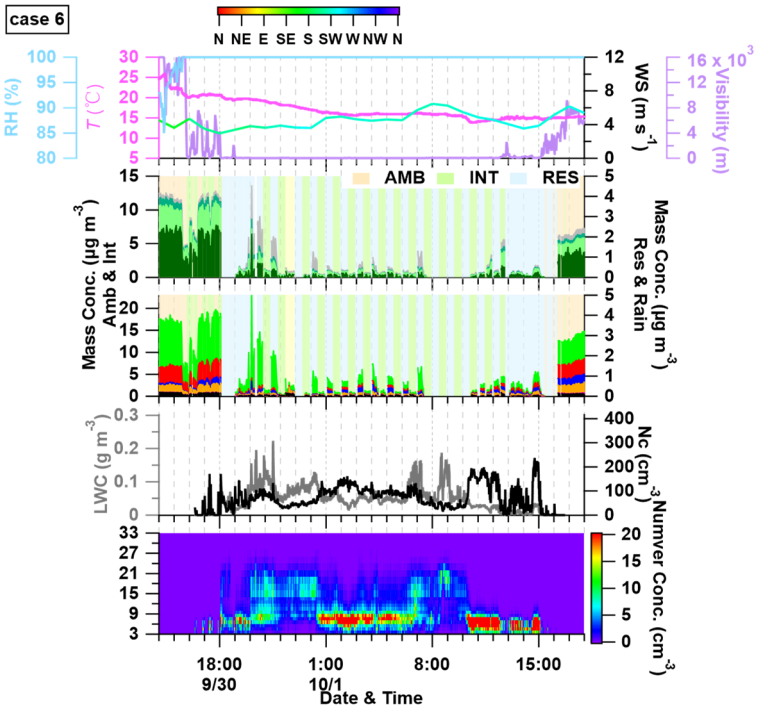

Figure S14: Same as Fig. S12, but for cloud case 6 in 2023.

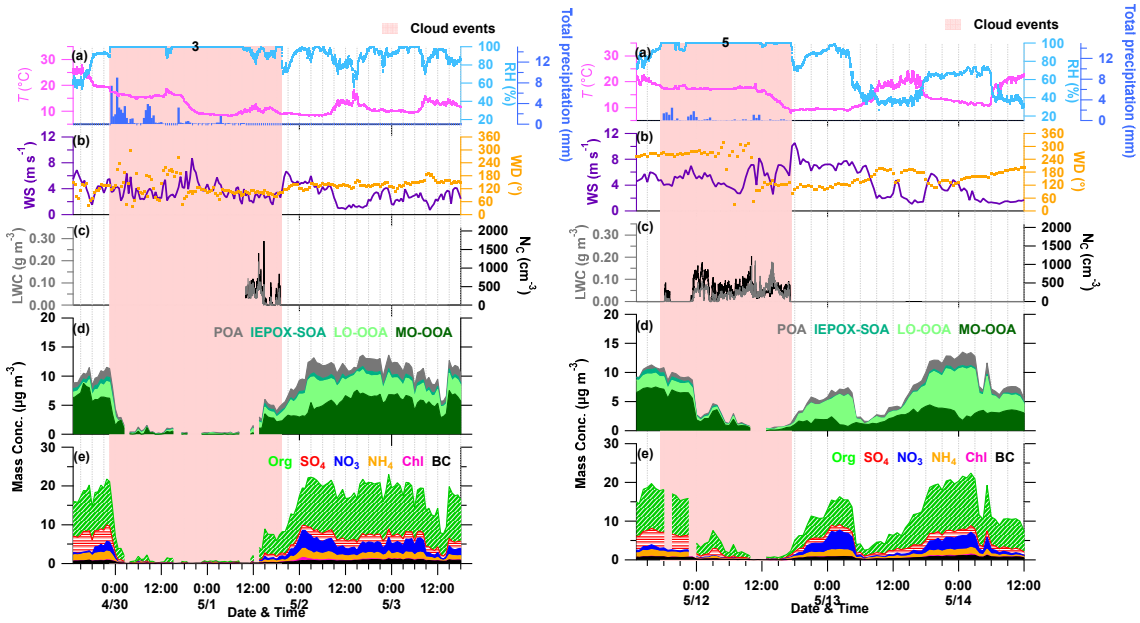

Figure S15: Same as Fig. S12, but for cloud case 3 and case 5 in 2024.

Table S1: Description of nine cloud events sampled during the measurement in 2023.

Index	Pre-cloud (AMB)	During cloud (RES and/or INT)	After cloud (AMB)	Duration (h)	precipitation	INT	Sources
Case 1	/	9.14 09:49-17:55	9.14 23:37-9.15 05:00	8.1	9.14 17:57-23:35	✓	East
Case 2	9.21 10:00-17:57	9.21 17:59-9.23 09:33	9.23 09:35-15:39	39.6		✓	East
Case 3	9.23 10:49-16:53	9.23 16:55-9.24 11:19	9.24 11:21-15:00	18.4	/	✓	East
Case 4	9.24 20:00-22:04	9.24 22:06-9.25 7:14	9.25 07:16-10:00	9.1	/	/	East
Case 5	9.25 18:48-20:46	9.25 20:48-9:26 09:43	9.26 09:45-12:00	12.9	/	/	East
Case 6	9.30 14:00-17:50	9.30 18:02-10.1 15:24	10.1 16:20-10.1 18:00	21.3	9.30 22:20-22:54	✓	North
Case 7	10.3 21:00-10.4 00:16	10.4 11:28-10.5 03:57	10.5 3:59-10.5 09:00	16.5	10.4 05:30-10.4 11:26	✓	North
Case 8	10.13 20:00-21:57	10:13 21:59-10.14 09:11	10.14 09:13-10:00	11.2	/	/	West
Case 9	10.14 21:00-22:31	10.14 22:33-10.15 08:40	10.15 08:42-12:00	10.1	/	/	West

Table S2: Description of seven cloud events sampled during the measurement in 2024.

Index	Pre-cloud (AMB)	During cloud (RES and INT)	After cloud (AMB)	Duration (h)	Precipitation	Sources
Case 1	4.20 13:11-14:11	4.20 14:11-4.23 18:44	4.23 18:44- 19:44	76.6 h	4.21 23:30-4.22 02:00	South
Case 2	4.27 17:48- 18:48	4.27 18:48-4.28 09:46	4.28 09:46-10:46	15.0 h	/	South
Case 3	4.29 21:30-22:30	4.29 22:30-5.1 19:22	5.1 19:22-20:22	44.9 h	4.29 23:00-4.30 04:30, 4.30 07:30-10:00	West
Case 4	5.3 19:00-20:00	5.3 20:00-5.6 7:40	5.6 07:40-08:40	59.7 h	5.4 02:00-07:30, 12:00-16:30, 5.5 01:30-03:00, 05:30-10:00	West
Case 5	5.11 16:20-17:20	5.11 17:20-5.12 17:20	5.12 17:20-18:20	24.0 h	5.11 18:00-19:30, 22:30-23:30	North
Case 6	5.20 12:55-13:55	5.20 13:55-5.23 07:20	5.23 07:20-08:20	65.4 h	5.21 09:30-14:30, 16:30-19:30	East
Case 7	5.27 07:20-08:20	5.27 08:20-5.28 08:00	5.28 08:00-09:00	23.7 h	5.27 10:30-16:30	North

Table S3: Comparison of main particle chemical components and meteorological parameters (average ± standard deviation) during field campaigns in 2023 and 2024

Item		2023	2024
RES species ($\mu g\ m^{-3}$)	Org	0.49 ± 0.42	0.66 ± 0.60
	SO_4	0.09 ± 0.06	0.21 ± 0.26
	NO_3	0.11 ± 0.09	0.15 ± 0.17
	NH_4	0.07 ± 0.06	0.11 ± 0.11
	BC	0.02 ± 0.02	0.03 ± 0.03
	POA	0.11 ± 0.17	0.08 ± 0.09
	IEPOX-SOA	0.06 ± 0.09	0.06 ± 0.05
	LO-OOA	0.17 ± 0.11	0.22 ± 0.23
	MO-OOA	0.20 ± 0.15	0.28 ± 0.21
INT species ($\mu g\ m^{-3}$)	Org	1.85 ± 1.38	3.20 ± 1.60
	SO_4	0.20 ± 0.24	0.92 ± 0.43
	NO_3	0.12 ± 0.23	0.35 ± 0.26
	NH_4	0.12 ± 0.25	0.42 ± 0.16
	BC	0.25 ± 0.10	0.25 ± 0.17
	POA	0.34 ± 0.20	0.45 ± 0.27
	IEPOX-SOA	0.29 ± 0.27	0.22 ± 0.09
	LO-OOA	0.93 ± 0.79	0.63 ± 0.39
	MO-OOA	0.58 ± 0.50	1.83 ± 0.92
AMB species ($\mu g\ m^{-3}$)	Org	6.51 ± 3.14	6.20 ± 3.32
	SO_4	1.82 ± 1.11	1.82 ± 1.00
	NO_3	0.96 ± 1.03	0.74 ± 0.69
	NH_4	1.02 ± 0.70	0.80 ± 0.49
	BC	0.55 ± 0.29	0.47 ± 0.22
	POA	0.74 ± 0.33	0.79 ± 0.46
	IEPOX-SOA	0.62 ± 0.38	0.40 ± 0.26

	LO-OOA	2.68 ± 1.37	1.35 ± 0.82
	MO-OOA	3.00 ± 1.64	3.52 ± 1.92
Meteorological parameters	T (^{o}C)	18.1 ± 4.5	17.4 ± 4.3
	RH (%)	94.4 ± 10.6	82.3 ± 22.0
	WS (m s^{-1})	4.1 ± 2.2	3.9 ± 2.2
Cloud microphysical parameters	LWC	0.07 ± 0.05	0.04 ± 0.03
	N_c (cm^{-3})	109.9 ± 76.2	230.5 ± 174.6
	D_e (μm)	13.4 ± 5.4	8.2 ± 3.2

Table S4: Average scavenging efficiency (η) of different chemical components during cloud formation in 2023 and 2024

	η in 2023	η in 2024
Org	65.0	73.8
SO_4	84.7	79.2
NO_3	65.9	71.9
NH_4	86.5	73.9
BC	61.0	63.4
POA	46.3	58.6
IEPOX-SOA	64.5	75.0
LO-OOA	56.4	73.1
MO-OOA	81.7	74.6

References

Stein, A. F., Draxler, R. R., Rolph, G., Stunder, B., Cohen, M. D., and Ngan, F.: NOAA's HYSPLIT Atmospheric Transport and Dispersion Modeling System, Bulletin of the American Meteorological Society, 96, 2059-2077, 10.1175/BAMS-D-14-00110.1, 2015.

Wang, Y. Q.: MeteoInfo: GIS software for meteorological data visualization and analysis, Meteorological Applications, 21, 360-368, 10.1002/met.1345, 2014.